TRAFIKVERKET

RAPPORT

Utveckling mobil datafångst: Evaluation of testing methods for positioning modules

Projektnummer: FOI-projekt 5148

Dokumenttitel: Utveckling mobil datafångst: Evaluation of testing methods for positioning modules
Skapat av: Milan Horemuz och Patric Jansson, KTH
Dokumentdatum: 2013-12-30
Dokumenttyp: Rapport
DokumentID:
Ärendenummer:
Projektnummer: FOI-projekt 5148
Version: 1.0

Publiceringsdatum:
Utgivare: Trafikverket
Kontaktperson: Joakim Fransson
Uppdragsansvarig:
Tryck:
Distributör: Trafikverket, Adress, Post nr Ort, telefon: 0771-921 921

Contents

1. Introduction

This report was written as a part of the project “Utveckling mobil datafångst” FOI-projekt 5148 carried on at Royal Institute of Technology (KTH) in Stockholm. In the project, one report has been published (Jansson and Horemuž, 2013). This is the second and final report.

In this report we use terminology according to the Guide to Uncertainty in Measurements (GUM) (International Organization for Standardization, 2008).

1.1. Background and Goal

The mobile data collection has received much attention from researchers all over the world during the past 15 – 20 years. The result of this extensive work is a number of commercially available products, usually called mobile mapping systems (MMS), which are used for collection of geospatial data from cars or aircrafts. The heart of each MMS is the positioning module based on a combination of a GNSS receiver and an inertial navigation system (INS). The module determines the position and orientation of the platform. The platform is equipped with a mapping sensor, usually a laser scanner and/or one or more digital cameras. The accuracy of the collected data greatly depends on the accuracy of the positioning module.

The data delivered by the MMS is a point cloud of the area of interest. Each point in the point cloud has 3D coordinates expressed in a required reference system and eventually other attributes like intensity of returned signal or colour. The quality of the data depends on many factors. The term “quality” usually refers to completeness and accuracy of data. In this report we focus only on the accuracy aspect of the quality. The term “accuracy” depicts the degree of conformance between the “true” and measured quantity (coordinates, velocity and orientation).

There are three groups of uncertainty sources, which affect the accuracy of each individual point in the point cloud (Jansson and Horemuž , 2013):

- Uncertainty from positioning module, i.e. errors stemming from gyroscopes, accelerometers, GNSS and processing errors
- Uncertainty from mapping sensor, i.e. errors from laser scanner or cameras
- Environmental and calibration uncertainties, i.e. atmospheric influence and uncertainty in knowledge of the offset and relative orientation between IMU and mapping sensors and IMU and GNSS antenna.

The goal of this project is to describe and evaluate two field test methods to be used to verify the performance of a positioning module as part of a MMS.

1.2. Uncertainty for Positioning Modules

It is possible to assess the accuracy of the positioning module analytically, i.e. to compute the expected accuracy taking into account the contribution from all possible error sources. In this case we do not know the “true” values; therefore, we refer to this analysis as uncertainty, or precision analysis. The result of the analysis is expected standard uncertainty (expressed in term of standard deviation) of the determined quantities, in our case the coordinates, velocity and orientation of mapping sensor and coordinates of mapped points.

In Jansson and Horemuž (2013) an uncertainty analysis is performed analytically. They present achievable standard uncertainties in the orientation for GNSS aided tactical and navigational grade INS. The analytically computed uncertainties are slightly more optimistic than for example those published by Skaloud (2002), which is expected, since the analytical computations take into account only the sensor noise and ideal GNSS observations. In practice, we will never get these ideal conditions and the results will be affected by other error sources, namely unmodelled GNSS systematic effects (mainly multipath and atmosphere) and errors coming from processing algorithm limitations. These limitations are caused by approximations that are necessary to apply when integrating the output from gyroscopes and accelerometers. Another cause of these limitations is the fact that the inertial sensors do not measure the acceleration and rotation rate continuously, but discretely, usually with frequency 100 – 300 Hz. These limitations can cause errors in both position and orientation and they are especially pronounced in high dynamics environment, e.g. sudden manoeuvres or vibrations caused by vehicle's engine (Jansson and Horemuž, 2013).

In order to verify the performance of a GNSS/INS positioning module in a production environment and to get more realistic uncertainty values we need field test methods.

1.3. Test Methods for Positioning Modules

As we could see from the previous discussion, a MMS is a complex system with many possible error sources. The analytical study can predict the precision (or uncertainty) but cannot guarantee the accuracy of the results. This can be compared with other surveying methods, e.g. measurements with RTK or total station, where the accuracy is verified experimentally either by measuring on known points (calibration baselines) or by comparing the measurements to those performed by other instrument/methods. Similar principles can be applied also to accuracy verification of positioning modules.

There are several alternatives how to verify the performance of a GNSS/INS positioning module (Jansson and Horemuž, 2013):

- Laboratory testing
- Field testing using an independent positioning system – direct method
- Field testing using the mapping sensors – the indirect method

Laboratory testing is not considered because this project is aiming at field test methods. In the direct method (field testing using an independent positioning system), position and orientation of the positioning module is determined directly by an independent method. By "direct" determination we mean that the position and orientation of the platform itself is measured. The independent method should be accurate and reliable, so that any gross or systematic error can be detected. "Indirect" determination refers to methods where the position of surveyed objects (by MMS) is used to determine the accuracy of the positioning module. In this case, however, the position of surveyed objects is also influenced by errors in the mapping sensor which have to be taken into consideration.

The direct method is in principle identical to laboratory testing described in Jansson and Horemuž (2013). The main difference is that the testing is done in field in a production environment and that the reference ("true") values are not determined with as high accuracy as in the laboratory testing.

In the indirect method (field testing using the mapping sensors), the mapping sensors are attached to the positioning module and they measure the surrounding objects. Then it is possible to compare measured coordinates of the objects with the coordinates measured by some other, preferably more accurate method/instrument (Jansson and Horemuž, 2013).

In the following sections, we will describe and evaluate the direct and the indirect field test methods.

2. Measurements

The goal of the measurements was to evaluate direct and indirect test methods for positioning modules. The purpose of these test methods is to determine the precision of the platform's position and orientation. The direct method uses total station (TS) observations towards prisms mounted onto platform to determine its position and orientation. The indirect method makes use of surveyed objects, which were scanned by the laser scanner mounted on the platform.

2.1. Location of Test Measurements

The test measurements were performed on November 6, 2013 in Gärdet, Stockholm. The road is marked by the red line in Figure 1, the length is approximately 500 m. The chosen area is ideal for GNSS observations as there are no obstacles blocking the satellite signals.

Figure 1. Test area in Gärdet, Stockholm.

2.2. Instruments

We used the mobile mapping system GeoTracker (Figure 2) provided by company WSP. Its positioning module consists of a geodetic dual frequency Novatel ProPak-V3 GNSS receiver, inertial navigation system Inertial+ and an odometer. According to the specifications published by the manufacturer[1], Inertial+ can determine roll and pitch with standard uncertainty 0.03° and heading 0.1°. These values are valid if the INS is supported by GNSS positions (0,5 s update) with positional standard uncertainty of 2 cm. To be able to apply the direct testing method, we installed 5 prisms onto the platform: 4 prisms at the corners and 1 prism under the GNSS antenna – see Figure 2. The prisms were surveyed by three total stations Trimble S3, which were established with help of Trimble R4 GNSS receivers using RUFRIS method (Andersson 2012). GeoTracker is equipped with four SICK LMS511 PRO laser scanners, which serve as mapping sensors. According to the manufacturer's specification "statistical error (1σ) using high resolution in 1 – 10 m range is ±7 mm".

Figure 2. Mobile mapping system GeoTracker.

2.3. Measuring Procedure

The car drove the road six times and in each run we collected data necessary for both test methods. Before we started the driving, we set up:

- 8 targets to be scanned (MT1 – MT8)
- 3 total stations (TS1 – TS3)
- 2 reference GNSS receivers (REFT, REFL)

The locations of the set-ups are shown Figure 3. They were marked by wooden stakes in the ground.

[1] http://www.oxts.com/products/inertial/

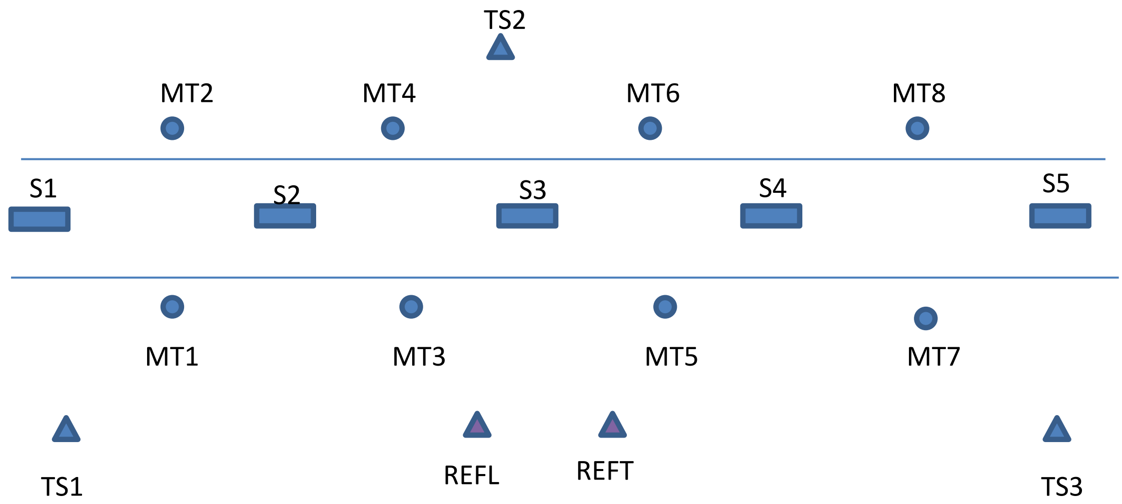

Figure 3. Location of the targets (MT), total stations (TS), reference GNSS receivers (REFL, REFT) and stops (S) of the car.

The total stations were established by the RUFRIS method, i.e. we used RTK method to determine the coordinates of prisms, which were measured by the total station. At least 19 such measurements were used for the establishment of the total stations and they were distributed around the respective total station and placed up to 400 m distance from the TS. RTK reference receiver REFT (Trimble) was used for RUFRIS measurements and the computation was done in real time, but raw GNSS observation from the reference and roving receivers were stored and hence post processing was possible. After the establishment of TS we surveyed all targets (MT) by all 3 TS and we also measured horizontal directions towards the TS, i.e. we aimed at the string of plumb attached underneath of TS tripod. We used two types of targets. The size of the first type is 24 x 16 cm (Figure 4 left) and the size of the second is 10 x 10 cm (Figure 4 right) – this type was used only on one point – MT3.

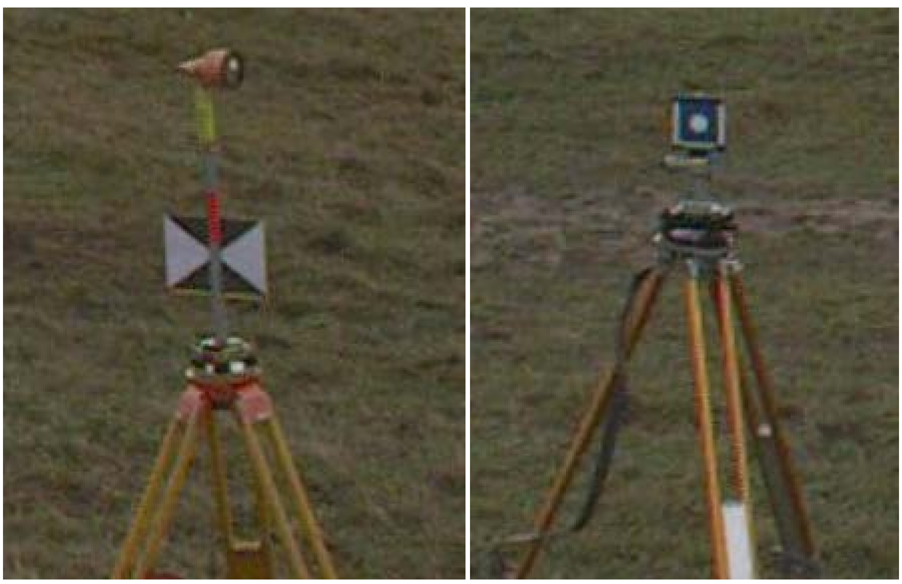

Figure 4. Two types of targets. Left figure: MT1, MT2, MT4 – MT8, right figure MT3 .

After these measurements we could start to drive the car. Each run started with ca 50 m driving and then the car stopped either at S1 or at S6, depending on the direction of the run. When the car stopped, the TS operators surveyed all visible prisms mounted on the platform and the operator in the car marked the stop in the trajectory data. Numbering of the prisms on the platform is shown in Figure 5. Since we measured every prism in every run 5 times, we denoted the prisms as KiSjPk, where Ki (i = 1 ... 6) denotes run (Körning), Sj (j = 1 ... 5) denotes stop and Pk (k= 1 ... 5) denotes prism. For example, when we measured prism P5 in the first run and the first stop, it was named as K1S1P5. When all operators completed the measurements, the car moved to the next stop (S2 or S4) and the prisms were again surveyed by all 3 TS. This procedure was repeated in the remaining stops. It took 13 – 16 minutes to complete one run.

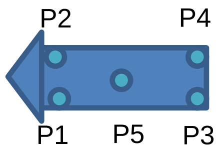

Figure 5. Numbering of prisms on the mobile platform. Arrow indicates driving direction.

After we completed 6 runs, we tested tracking the platform by TS. The goal with this test was to verify whether it is possible to determine the position and orientation of the platform without necessity of stopping the car. Since the TS was unable to "snap" on a prism if there were more visible prisms, we had to remove all but one prism, i.e. only prism 5 was tracked. The tracking experiment was performed only in one run.

As the last steps in the measuring procedure, we verified the stability of all set-ups by checking the centring and we performed TS observation between station points and towards point REFT. We also performed levelling between TS points and REFT.

3. Computations

3.1. Reference system

All computations were done in reference system SWEREF 99 18 00, geoid model SWEN08_RH2000. Our measurements were connected to this system by baseline between SWEPOS point MOSE and our GNSS station REFL. We used ca 3 hours of static GNSS observations to compute this ca 3 km baseline, which gave 1 mm horizontal and 5 mm vertical standard uncertainty (68%). The reference station REFL was used for the GNNS/INS processing in GeoTracker system, i.e. the platform's trajectory and the point cloud is georeferenced relative to this point. The TS observations are georeferenced relative to REFT point located ca 10 m from REFL. REFT was determined by processing baseline REFL-REFT using ca 1.2 hour static GNSS observations, which gave 0.5 mm horizontal and 1 mm vertical standard uncertainty (68%).

Please note, that the choice of reference system does not affect the tested methods. In principle we can choose any system; it is only important that all kind of observations are processed in the chosen system.

3.2. Processing of TS measurements

The TS observations and all GNSS observations performed relative to REFT were processed in software Trimble Business Centre (TBC). All RTK observations were re-computed in post-processing mode using REFT as reference (fixed) point. Then all RUFRIS and TS observations towards P, MT and TS points were adjusted together. The precision of all P and MT points was approximately equal, since all points were measured from 3 TS with approximately equal geometry.

Precision of coordinates of P1 – P5, MT1 – MT8
Standard uncertainty of horizontal and vertical coordinates determined by least-squares adjustment is $u(E_{TS}) = u(N_{TS}) = 2$ mm and $u(H_{TS}) = 1$ mm.

3.3. Processing of platform's observations

The processing of observations coming from the platform's sensors was performed by WSP in software GeoTracker Office (bilskanning.se). The result of this processing was the trajectory of the platform and georeferenced point cloud. The trajectory is given in form of coordinates (N, E, H in meters), orientation angles (roll, pitch, heading in degrees) and their standard uncertainties. The coordinates of prism P5 and the orientation angles for all stops are given in Appendix 6. These values are extracted from the trajectory file for the time instance immediately after the stop.

Precision of trajectory determined by GeoTracker
Standard uncertainty of horizontal and vertical coordinates is 2 - 3 mm and 5 mm respectively. Standard uncertainty of roll and pitch is 0.01˚ and of heading 0.1˚. These values were reported by software.

Another deliverable from the mobile platform was georeferenced point cloud, where the targets MT are visible. The centre coordinates of the targets were extracted manually: the operator identified all points belonging to the target and fitted a rectangular patch to them. The centre point of the patch was considered as MT point. Moreover, we extracted even coordinates of the prisms mounted on top of the targets wherever it was possible – see Figure 6. The extracted coordinates are reported in Appendix 4.

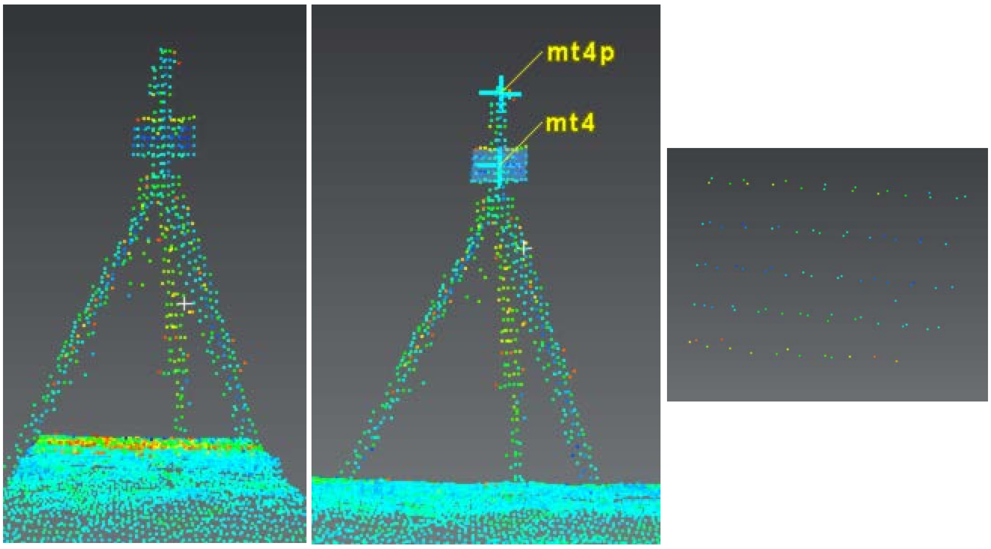

Figure 6. Determination of coordinates of MT points from point cloud.

Since the distance between individual laser points on the target was ca 2 cm in longitudinal direction and ca 4 cm vertically, we estimate that the standard uncertainty of the extracting procedure is about 1 cm longitudinally, 2 cm vertically and 0.5 cm transversally.

3.4. Determination of platform's orientation by TS observations

The orientation of the platform is described by a rotation matrix between the platform's and a horizontal coordinate system. Generally a rotation matrix between two frames (coordinate systems) a and b is given as:

$$\mathbf{R}_a^b = \begin{bmatrix} \cos(h)\cos(p) & \sin(h)\cos(p) & -\sin(p) \\ -\sin(h)\cos(r)+\cos(h)\sin(p)\sin(r) & \cos(h)\cos(r)+\sin(h)\sin(p)\sin(r) & \cos(p)\sin(r) \\ \sin(h)\sin(r)+\cos(h)\sin(p)\cos(r) & -\cos(h)\sin(r)+\sin(h)\sin(p)\cos(r) & \cos(p)\cos(r) \end{bmatrix} \quad (1)$$

where r, p, h are orientation angles, i.e. the amount of rotation of a frame around its around x, y, z axes. In our case we use the horizontal system SWEREF99 18 00, denoted as **n-frame** and the order of axes is Northing, Easting, Down, where Down is minus height (-H). We have two coordinate frames attached to the platform: one is defined by the sensitive axes of the INS (**b-frame**) and the other one is defined by the prisms (P1 – P5) mounted onto the platform; we will call it **t-frame** and its definition is explained in Figure 7.

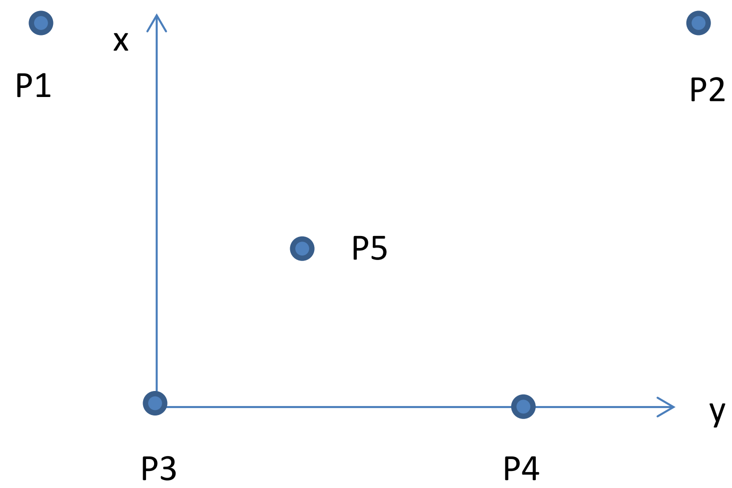

Figure 7. Definition of t-frame: origin in P3, y axis passes P4, z axis points downwards; z coordinate of P1, P3 and P4 is equal to zero.

The orientation angles between frames n and b are called roll, pitch and heading (rotation matrix $\mathbf{R}_n^b$) and we will refer to the orientation angles between n- and t-frames (rotation matrix $\mathbf{R}_n^t$) as roll_t, pitch_t and heading_t.

The coordinates of P1 – P5 prisms in t-frame were computed in two steps. In the first step we defined t-frame coordinates of P3, P4 and P1 computed for each stop as:

	x	y	z
P1	$d_{31} \cos \varphi_{31}$	$d_{31} \sin \varphi_{31}$	0,000
P3	0,000	0,000	0,000
P4	0,000	d_{34}	0,000

where

d_{31}, d_{34} – slope distance between P3 and P1 (resp. P4) computed from n-frame coordinates determined by TS observations

φ_{31} – bearing from P3 to P1 computed in t-frame using distances d_{31}, d_{34} and d_{41} computed as slope distances in n-frame. (Solving triangle P1-P3-P4 using cosine rule.)

The coordinates of P2 and P5 were computed by Helmert transformation

$$\mathbf{X}^t = \mathbf{T}^t + \mathbf{R}_n^t \mathbf{X}^n \qquad (2)$$

where $\mathbf{X}^t$ is vector containing t-frame coordinates, $\mathbf{X}^n$ is vector containing n-frame coordinates and $\mathbf{T}^t$ and $\mathbf{R}_n^t$ are translation vector and rotation matrix estimated by the least-square method using three common points (P3, P4, P1). The final t-frame coordinates of all prisms (P1 – P5) were computed as average from all stops, see Table 1.

Table 1. t-frame coordinates of prisms. Their standard uncertainties are smaller than 0,5 mm.

	x [m]	y [m]	z [m]
P1	1,618	-0,397	0,000
P2	1,624	1,180	0,001
P3	0,000	0,000	0,000
P4	0,000	0,791	0,000
P5	0,440	0,290	-0,286

In the second step we used these averaged coordinates to compute the transformation parameters between n- and t-frame ($\mathbf{T}^t$ and orientation angles roll_t, pitch_t, yaw_t, i.e. rotation matrix $\mathbf{R}_n^t$ from Equation (2)). We computed the transformation parameters and their standard uncertainty by LSQ method for each stop; they are shown in Appendix 1.

Precision of orientation angles determined by TS

Mean standard uncertainty of the orientation angles is 0.062, 0.049, 0.039 degrees for roll_t, pitch_t, yaw_t respectively.

3.5. Orientation of t-frame with respect to b-frame

The orientation of t-frame relative to b-frame must be constant, since both frames are firmly mounted to the platform. It can be computed as:

$$\mathbf{R}_t^b = \mathbf{R}_n^b \mathbf{R}_t^n \tag{3}$$

where $\mathbf{R}_t^n = \left(\mathbf{R}_n^t\right)^T$. The orientation angles between t- and b-frame are computed as

$$\begin{aligned} r_x &= \arctan \frac{R_{23}}{R_{33}} \\ r_y &= \arcsin\left(-R_{13}\right) \\ rz &= \arctan \frac{R_{12}}{R_{11}} \end{aligned} \tag{4}$$

where R_{ij} denotes an element from $\mathbf{R}_t^b$ matrix, i denotes row and j column. We computed matrix $\mathbf{R}_t^b$ 30 times, i.e. for each stop in every run. The computed orientation angles are given in Appendix 2. Standard uncertainty of orientation angles (computed as standard deviation): $u(r_x) = 0.061^\circ$, $u(r_y) = 0.064^\circ$, $u(r_z) = 0.095^\circ$.

4. Analysis

4.1. Direct method

Position and orientation of the platform determined by TS observations is used to verify the results obtained by the platform's positioning module. As the t-frame realised by the prisms does not coincide with the module's b-frame, we cannot compare the orientation angles directly, but we can analyse the variation of the orientation angles between t- and b-frames, r_x, r_y and r_z. The variation is caused by the uncertainty in TS observations as well as by uncertainty in positioning module, so we can write

$$\begin{aligned} u\left(r_x\right) &= \sqrt{u^2\left(roll\right) + u^2\left(roll\_t\right)} \\ u\left(r_y\right) &= \sqrt{u^2\left(pitch\right) + u^2\left(pitch\_t\right)} \\ u\left(r_z\right) &= \sqrt{u^2\left(heading\right) + u^2\left(heading\_t\right)} \end{aligned} \tag{5}$$

or

$$\begin{aligned} u\left(roll\right) &= \sqrt{u^2\left(r_x\right) - u^2\left(roll\_t\right)} \\ u\left(pitch\right) &= \sqrt{u^2\left(r_y\right) - u^2\left(pitch\_t\right)} \\ u\left(heading\right) &= \sqrt{u^2\left(r_z\right) - u^2\left(heading\_t\right)} \end{aligned} \tag{6}$$

These equations are valid only for small rotation angles between t- and b-frame and for theoretical standard uncertainties determined from infinite number of observations, which follow normal distribution. If we enter results from our test measurements (see Appendix 1 and 2) into Equation (6), we get the following standard uncertainties:

$$\begin{aligned} u\left(roll\right) &= \sqrt{0.061^2 - 0.063^2} \approx 0° \\ u\left(pitch\right) &= \sqrt{0.064^2 - 0.048^2} = 0.042° \\ u\left(heading\right) &= \sqrt{0.095^2 - 0.039^2} = 0.087° \end{aligned} \tag{7}$$

which can be compared with the uncertainties specified by the manufacturer of the positioning module: 0.03° for roll and pitch and 0.1° for heading.

As we can see from the equation for u(roll), we can get a negative number under the square root, due to the finite number of observations used to compute the standard uncertainties.

The position obtained by TS is compared to the position from the positioning module in Appendix 3. Average value of differences in N and E coordinates is 1 mm and standard uncertainty of the average u(average) = 1 mm. For height, the average difference is 10 mm and u(average) = 1 mm, which indicates a possible systematic effect of 10 mm in height determination. A possible explanation is the effect of GNSS configuration (RUFRIS was performed ca 2 hours earlier then car driving) or an error in antenna height measurement.

Standard uncertainty of coordinate differences is u(diffE) = 5 mm, u(diffN) = 6 mm and u(diffH) = 5 mm.

The standard uncertainties in coordinate differences are computed according to the following equation:

$$u(x)=\sqrt{\frac{\sum_{i=1}^{n}\left(\overline{x}-x_{i}\right)}{n-1}} \tag{8}$$

and standard uncertainty in the average

$$u(\overline{x})=\frac{u(x)}{\sqrt{n}} \tag{9}$$

where x_i is a coordinate difference, $\overline{x}$ is average of the differences and n is number of differences.

Standard uncertainties of the coordinate differences are related to the TS and positioning module (PM) standard uncertainties as:

$$\begin{aligned} u\left(diffE\right)&=\sqrt{u^{2}\left(E_{TS}\right)+u^{2}\left(E_{PM}\right)}\\ u\left(diffN\right)&=\sqrt{u^{2}\left(N_{TS}\right)+u^{2}\left(N_{PM}\right)}\\ u\left(diffH\right)&=\sqrt{u^{2}\left(H_{TS}\right)+u^{2}\left(H_{PM}\right)} \end{aligned} \tag{10}$$

or

$$\begin{aligned} u\left(E_{PM}\right)&=\sqrt{u^{2}\left(diffE\right)-u^{2}\left(E_{TS}\right)}\\ u\left(N_{PM}\right)&=\sqrt{u^{2}\left(diffN\right)-u^{2}\left(N_{TS}\right)}.\\ u\left(H_{PM}\right)&=\sqrt{u^{2}\left(diffH\right)-u^{2}\left(H_{TS}\right)} \end{aligned} \tag{11}$$

Using our results (see section 3.2) we obtain:

$$\begin{aligned} u\left(E_{PM}\right)&=\sqrt{5^{2}-2^{2}}=4.6\ \text{mm}\\ u\left(N_{PM}\right)&=\sqrt{6^{2}-2^{2}}=5.7\ \text{mm}\\ u\left(H_{PM}\right)&=\sqrt{5^{2}-1^{2}}=4.9\ \text{mm} \end{aligned} \tag{12}$$

which can be compared with positioning standard uncertainty of 20 mm specified by the manufacturer.

Based on our results, we can conclude that the positioning module was performing in accordance with the specifications.

4.2. Indirect method

In this method we use the differences between coordinates of the targets determined by TS and MMS. To be able to use the coordinate differences for the evaluation of the platform's performance, we need to transform them into a coordinate system aligned with the driving direction (Figure 8), i.e. we compute longitudinal and transverse difference as

$$\begin{aligned} diffT &= diff \sin \alpha \\ diffL &= diff \cos \alpha \end{aligned} \tag{13}$$

where

$$\begin{aligned} diff &= \sqrt{diffE^2 + diffN^2} \\ \alpha &= \varphi_r - \varphi_{diff} \\ \varphi_{diff} &= \arctan \frac{diffE}{diffN} \end{aligned} \tag{14}$$

$\varphi_r = 110^\circ$ is the bearing of the road.

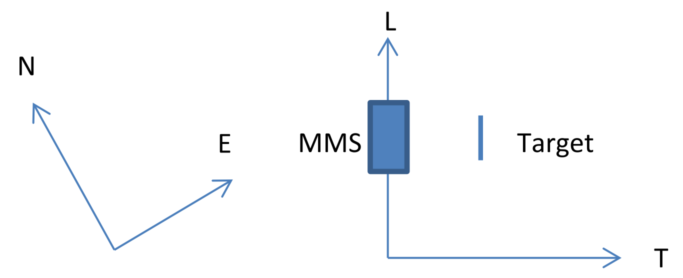

Figure 8. Definition of longitudinal coordinate system.

Since the targets are located at approximately the same height as the mobile platform, the standard uncertainties of the coordinate differences in longitudinal coordinate system can be expressed by the following simplified equations:

$$\begin{aligned} u(diffL) &= \sqrt{u^2(GNSS\_NE) + u^2(ident\_L) + u^2(sync) + \left(du(heading)\right)^2} \\ u(diffT) &= \sqrt{u^2(GNSS\_NE) + u^2(ident\_T) + u^2(dist)} \\ u(diffH) &= \sqrt{u^2(GNSS\_H) + u^2(ident\_H) + \left(du(roll + laser)\right)^2} \end{aligned} \tag{15}$$

where d is distance between the platform and the target, we consider a mean distance d = 7 m. u(GNSS) is standard uncertainty in N, E and H coordinates determined by GNSS/INS, we consider mean values taken from Appendix 6: u(GNSS_NE) = 3 mm and u(GNSS_H) = 5 mm. u(sync) is uncertainty in longitudinal position of the laser scanner due to uncertainty in synchronisation between positioning module and the laser scanner. We do not have any information about the synchronisation uncertainty so we consider an empirical value u(sync) = 1 cm. u(ident_L) and u(ident_H) is standard uncertainty of target identification in longitudinal and vertical direction, which depends on the density of the point cloud. We consider u(ident_L) = 1 cm and u(ident_H) = 2 cm (see section 3.2). u(ident_T) is standard uncertainty of target identification in transversal direction, which depends on the number of scanned points on the target that were used to fit a planar patch. Based on the “fitting quality” descriptor obtained in Cyclone software when fitting the patches, we consider u(ident_T) = 3 mm. Uncertainty in height determination is influenced both by laser scanner's angular precision as well as by the precision in roll determination. The scanner's angular precision is not stated explicitly in the specifications, but usually the laser scanner's angular precision is ca 10 times higher than the precision of roll, therefore we can state that u(roll+laser) ≈ u(roll). By rearranging Equation (15) and using values u(diffL)= 0.023 m, u(diffT) = 0.005 m and u(diffH) = 0.008 m from Appendix 5 we get:

$$\begin{aligned} u\left(heading\right) &= \sqrt{0.023^2 - 0.003^2 - 0.01^2 - 0.01^2} \ / \ 7 = 0.15° \\ u\left(dist\right) &= \sqrt{0.005^2 - 0.003^2 - 0.003^2} \ = 0.002 \text{ m} \\ u\left(roll\right) &= \sqrt{0.008^2 - 0.005^2} \ / \ 7 = 0.05° \end{aligned} \tag{16}$$

Please note that we set u(ident_H) = 0, when computing u(roll) to avoid negative number under square root, so u(roll) < 0.05°. u(pitch) is not possible to determine with given experimental set up. To be able to evaluate even u(pitch), we would need to scan some targets at different heights.

Based on the results in Equation (16), we can conclude that the positioning module was performing in accordance with specifications.

5. Conclusions

The result of a test of positioning module should confirm or refute that the positioning module is performing in accordance with the specifications. The goal of this report was to evaluate two testing methods: direct and indirect. Both methods are capable to evaluate the performance of the positioning module, but both have advantages and disadvantages – see summary in Table 2. The main advantage of the direct method is that it tests precision of all parameters (three coordinates and three orientation angles) directly, i.e. TS measurements are compared with the output of the positioning module. On the other hand, in the indirect method we are using the output from a mapping sensor – laser scanner, which introduces a number of factors influencing the results and often it is difficult to quantify this influence. In the indirect approach, the centre of the scanned targets must be identified; it is difficult to assign a standard uncertainty of this procedure since it can vary significantly depending on the size and material of the target and on its distance from the MMS. Another uncertain factor is the synchronisation between the positioning module and the laser scanner. Moreover, determined uncertainty in the orientation angles depends on the uncertainty in GNSS coordinates, which can vary significantly from place to place. The main disadvantage of the direct method is the time consumption and necessity of two or three operators. In our test measurements we used 3 TS, hence 3 operators, which provided a homogeneous geometry for whole trajectory. In principle, one TS would suffice, but then it would not be possible to identify eventual gross errors, therefore we recommend at least 2 total stations.

Table 2. Summary of main properties of the direct and indirect methods.

Direct	**Indirect**
More complicated and time consuming procedure: necessary to mount prisms onto the platform, 2 -3 operators for TS are required,	Simpler procedure: a fixed test field can be re-used, no operators required
Tests all parameters: 3 coordinates and 3 orientation angles	Pitch is difficult to test: high/low located targets are necessary
Tests all parameters directly	Mapping sensor is involved, which introduces a number of effects that influence the test results. Difficult to assign an uncertainty for these effects (synchronisation, target identification)
Car must stop when taking TS measurements	Car drives continuously
Suitable for testing the positioning module	Suitable for testing whole MMS

The indirect method is much less time consuming, especially in the case when a test field is already established. Then the car just drives through the test field. This method is suitable for testing the overall performance of the MMS, but less suitable for testing the performance of the positioning module only.

An improvement of the direct method would be using the tracking function of TS, i.e. TS would measure the trajectory of the prism continuously, without necessity of stopping the car. According to our experience, this is not a viable method, since the TS could not track a chosen prism, if there were more visible prisms on the platform; the TS "jumped" between prisms more or less randomly. We also tried to cover all but one prism. In this case the TS could track the prism successfully, but one prism is not sufficient to determine the orientation angles. Moreover, it was not possible to establish synchronisation between TS and platform's observation.

We should point out that the conclusions drawn from the tests are valid for the particular conditions during the test measurements, which can be significantly different in the actual production environment.

6. References

Andersson, J. V. (2012). Underlag till metodbeskrivning RUFRIS, Trafikverket.

International Organization for Standardization (2008). ISO/IEC Guide 98-3:2008 ”Uncertainty of Measurement -- Part 3: Guide to the Expression of Uncertainty in Measurement (GUM:1995)”

Jansson, P. and M. Horemuž (2013). Methods for Accuracy Verification of Positioning Module, Rapport 2013:008, ISBN: 978-91-7467-452-1, Trafikverket.

Skaloud, J. (2002) Direct Georeferencing in Aerial Photogrammetric Mapping, in Photogrammetric Engineering & Remote Sensing, p. 207-210.

Appendix 1

t-frame coordinates obtained by transformation from n-frame to mean coordinates computed in step 1.

	Prism 1			Prism 2		
	x	y	z	x	y	z
k1s1p1	-0,398	1,619	0,002	1,181	1,625	-0,003
k1s2p1	-0,396	1,620	-0,001	1,179	1,625	0,000
k1s3p1	-0,397	1,617	0,000	1,181	1,625	-0,001
k1s4p1	-0,397	1,618	0,000	1,181	1,625	-0,001
k1s5p1	-0,397	1,618	0,001	1,181	1,625	-0,001
k2s1p1	-0,397	1,617	0,000	1,180	1,624	-0,001
k2s2p1	-0,396	1,619	0,000	1,179	1,624	-0,001
k2s3p1	-0,397	1,620	0,000	1,179	1,624	-0,002
k2s4p1	-0,397	1,620	0,000	1,179	1,624	-0,001
k2s5p1	-0,397	1,619	-0,001	1,180	1,625	-0,001
k3s1p1	-0,396	1,619	0,001	1,179	1,623	-0,001
k3s2p1	-0,396	1,619	0,000	1,179	1,625	-0,001
k3s3p1	-0,397	1,618	0,000	1,180	1,624	0,000
k3s4p1	-0,396	1,618	0,000	1,179	1,625	0,000
k3s5p1	-0,397	1,618	0,000	1,180	1,623	0,000
k4s1p1	-0,397	1,617	0,000	1,180	1,624	-0,001
k4s2p1	-0,397	1,618	-0,001	1,180	1,624	0,000
k4s3p1	-0,397	1,618	0,000	1,181	1,626	-0,002
k4s4p1	-0,398	1,620	0,000	1,182	1,625	-0,001
k4s5p1	-0,396	1,618	-0,001	1,180	1,626	-0,001
k5s5p1	-0,396	1,619	0,000	1,179	1,625	-0,001
k5s2p1	-0,395	1,620	-0,001	1,178	1,625	0,000
k5s3p1	-0,398	1,618	0,000	1,181	1,623	0,000
k5s4p1	-0,399	1,618	0,000	1,182	1,624	0,000
k5s5p1	-0,397	1,618	0,001	1,181	1,623	-0,001
k6s1p1	-0,397	1,618	0,000	1,180	1,624	-0,001
k6s2p1	-0,396	1,618	0,000	1,180	1,625	-0,001
k6s3p1	-0,397	1,618	0,001	1,182	1,625	-0,002
k6s4p1	-0,397	1,619	0,000	1,180	1,624	-0,001
k6s5p1	-0,397	1,618	-0,001	1,180	1,626	-0,001

	Prism 3			Prism 4		
	x	y	z	x	y	z
k1s1p3	-0,002	0,001	-0,003	0,793	0,000	0,003
k1s2p3	-0,001	0,000	0,003	0,791	0,001	-0,001
k1s3p3	0,000	-0,001	0,000	0,790	-0,001	-0,001
k1s4p3	0,000	-0,001	0,000	0,791	0,000	0,000

k1s5p3	0,000	-0,002	0,000	0,792	-0,001	0,000
k2s1p3	-0,002	0,000	0,000	0,792	-0,001	-0,001
k2s2p3	0,000	0,000	0,000	0,792	-0,001	0,000
k2s3p3	0,002	0,002	-0,001	0,790	0,001	0,001
k2s4p3	-0,001	0,000	0,000	0,791	0,001	0,002
k2s5p3	-0,001	0,002	0,000	0,790	0,001	0,001
k3s1p3	0,001	0,001	0,000	0,792	0,000	0,001
k3s2p3	0,000	0,001	-0,001	0,791	-0,001	0,000
k3s3p3	0,003	0,000	0,001	0,789	0,000	0,000
k3s4p3	-0,001	-0,001	0,000	0,791	-0,001	-0,001
k3s5p3	-0,001	-0,002	0,001	0,793	-0,001	-0,001
k4s1p3	-0,001	0,000	0,000	0,792	0,000	0,000
k4s2p3	-0,002	0,000	0,000	0,791	0,000	0,000
k4s3p3	-0,002	0,000	-0,002	0,790	0,001	0,001
k4s4p3	0,002	-0,001	0,000	0,789	0,001	0,001
k4s5p3	0,000	0,001	0,001	0,789	0,001	-0,001
k5s1p3	0,000	0,001	0,001	0,792	-0,001	-0,001
k5s2p3	0,001	0,000	0,001	0,790	0,000	-0,001
k5s3p3	0,001	-0,001	0,001	0,789	0,000	-0,001
k5s4p3	0,000	-0,001	0,000	0,790	0,000	0,000
k5s5p3	0,003	-0,001	0,000	0,790	0,001	0,000
k6s1p3	0,000	0,001	-0,001	0,791	-0,001	-0,001
k6s2p3	0,000	0,000	0,000	0,791	-0,001	-0,001
k6s3p3	-0,002	0,000	-0,002	0,793	0,001	0,001
k6s4p3	0,002	0,000	0,000	0,791	0,001	-0,001
k6s5p3	-0,001	0,002	0,000	0,789	-0,001	0,001

		Prism 5	
	x	**y**	**z**
k1s1p5	0,289	0,438	0,287
k1s2p5	0,291	0,438	0,285
k1s3p5	0,289	0,443	0,286
k1s4p5	0,290	0,442	0,286
k1s5p5	0,288	0,443	0,286
k2s1p5	0,290	0,443	0,287
k2s2p5	0,290	0,441	0,286
k2s3p5	0,290	0,436	0,287
k2s4p5	0,293	0,439	0,284
k2s5p5	0,292	0,437	0,286
k3s1p5	0,289	0,440	0,285
k3s2p5	0,290	0,440	0,288
k3s3p5	0,290	0,442	0,285
k3s4p5	0,291	0,442	0,286
k3s5p5	0,289	0,445	0,285

k4s1p5	0,290	0,442	0,286
k4s2p5	0,292	0,441	0,286
k4s3p5	0,291	0,439	0,288
k4s4p5	0,290	0,439	0,285
k4s5p5	0,292	0,438	0,287
k5s1p5	0,290	0,440	0,286
k5s2p5	0,291	0,439	0,286
k5s3p5	0,291	0,443	0,285
k5s4p5	0,292	0,443	0,286
k5s5p5	0,287	0,443	0,286
k6s1p5	0,291	0,441	0,287
k6s2p5	0,290	0,441	0,287
k6s3p5	0,289	0,439	0,288
k6s4p5	0,289	0,439	0,288
k6s5p5	0,293	0,438	0,286

Average values

	x	y	z
P1	-0,397	1,618	0,000
P2	1,180	1,624	-0,001
P3	0,000	0,000	0,000
P4	0,791	0,000	0,000
P5	0,290	0,440	0,286

u(sample)

	x	y	z
P1	0,0008	0,0008	0,0005
P2	0,0010	0,0009	0,0007
P3	0,0013	0,0011	0,0011
P4	0,0013	0,0007	0,0010
P5	0,0014	0,0022	0,0011

u(average)

	x	y	z
P1	0,0001	0,0002	0,0001
P2	0,0002	0,0002	0,0001
P3	0,0002	0,0002	0,0002
P4	0,0002	0,0001	0,0002
P5	0,0003	0,0004	0,0002

Orientation angles between n-and t-frame computed by TS measurements

			roll_t	pitch_t	heading_t	u(roll_t)	u(pitch_t)	u(heading_t)
k1	s1	k1s1	-0,1164	-5,1627	109,3010	0,1046	0,0799	0,0645
k1	s2	k1s2	1,2161	-6,1730	109,9017	0,0692	0,0527	0,0426
k1	s3	k1s3	0,0672	-4,6206	110,4925	0,0602	0,0459	0,0371
k1	s4	k1s4	0,0305	-1,7273	110,5707	0,0409	0,0312	0,0252
k1	s5	k1s5	-0,5181	0,5319	110,4255	0,0588	0,0449	0,0362
k2	s1	k2s1	0,4793	-3,3222	-69,1517	0,0631	0,0481	0,0388
k2	s2	k2s2	0,0181	-2,0080	-69,0103	0,0328	0,0250	0,0202
k2	s3	k2s3	0,8932	-3,2332	-69,7893	0,0931	0,0709	0,0573
k2	s4	k2s4	0,3004	-7,0482	-69,5242	0,0734	0,0559	0,0452
k2	s5	k2s5	1,3706	-8,3551	-69,9997	0,0804	0,0613	0,0495
k3	s1	k3s1	1,1771	-4,9661	109,4521	0,0498	0,0379	0,0306
k3	s2	k3s2	0,9227	-6,1232	110,7807	0,0467	0,0356	0,0287
k3	s3	k3s3	0,3198	-4,6062	111,2303	0,0659	0,0502	0,0405
k3	s4	k3s4	0,2406	-1,7846	111,0139	0,0519	0,0395	0,0319
k3	s5	k3s5	-0,0481	0,7753	109,3871	0,0875	0,0667	0,0539
k4	s1	k4s1	1,9458	-3,4223	-69,6999	0,0283	0,0216	0,0174
k4	s2	k4s2	0,6843	-2,3066	-69,3055	0,0474	0,0362	0,0292
k4	s3	k4s3	1,2092	-3,4464	-69,0068	0,0643	0,0490	0,0396
k4	s4	k4s4	0,8837	-6,9492	-68,8677	0,0620	0,0472	0,0381
k4	s5	k4s5	2,1277	-8,4067	-70,1231	0,0645	0,0491	0,0397
k5	s1	k5s1	1,1942	-5,2512	109,7061	0,0500	0,0381	0,0307
k5	s2	k5s2	1,2070	-6,3442	110,2518	0,0563	0,0428	0,0346
k5	s3	k5s3	0,3578	-4,7586	110,6334	0,0787	0,0600	0,0485
k5	s4	k5s4	1,6106	-1,9050	109,9319	0,0748	0,0570	0,0460
k5	s5	k5s5	0,9684	0,3844	110,1513	0,0780	0,0595	0,0481
k6	s1	k6s1	1,8771	-3,3025	-69,3073	0,0481	0,0367	0,0296
k6	s2	k6s2	0,4768	-2,1754	-69,6005	0,0374	0,0285	0,0230
k6	s3	k6s3	1,0651	-3,3519	-69,9912	0,0737	0,0563	0,0454
k6	s4	k6s4	1,0334	-7,0393	-69,3846	0,0569	0,0433	0,0350
k6	s5	k6s5	1,9048	-8,4528	-71,0649	0,0827	0,0630	0,0509
					Mean	0,0627	0,0478	0,0386

Appendix 2

Orientation angles between t-frame and n-frame (r_x, r_y, r_z). Standard uncertainties in orientation angles are based on measurements from positioning module and total stations.

	Orientation angles [deg]		
	r_x	r_y	r_z
k1s1	-0,396	3,337	359,648
k1s2	-0,366	3,466	359,729
k1s3	-0,440	3,443	359,776
k1s4	-0,414	3,323	359,624
k1s5	-0,438	3,367	359,563
k2s1	-0,336	3,455	359,762
k2s2	-0,393	3,387	359,762
k2s3	-0,357	3,337	359,822
k2s4	-0,192	3,660	359,698
k2s5	-0,402	3,452	359,627
k3s1	-0,349	3,363	359,660
k3s2	-0,268	3,390	359,760
k3s3	-0,439	3,405	359,724
k3s4	-0,349	3,421	359,700
k3s5	-0,369	3,397	359,645
k4s1	-0,408	3,475	359,707
k4s2	-0,317	3,461	359,837
k4s3	-0,404	3,371	359,526
k4s4	-0,438	3,404	359,712
k4s5	-0,441	3,404	359,461
K5s1	-0,356	3,485	359,624
k5s2	-0,301	3,485	359,713
k5s3	-0,343	3,386	359,645
k5s4	-0,414	3,469	359,731
k5s5	-0,411	3,414	359,874
k6s1	-0,400	3,442	359,684
k6s2	-0,420	3,370	359,617
k6s3	-0,373	3,373	359,708
k6s4	-0,406	3,409	359,660
k6s5	-0,515	3,428	359,485
Average:	-0,382	3,419	359,683
u(sample)	0,061	0,064	0,095
u(average)	0,011	0,012	0,017

Appendix 3

Comparison of coordinates for prism no. 5 from positioning module and from total stations.

	GPS/INS			Totalstation					
Stop	**N**	**E**	**H**	**N**	**E**	**H**	**diff N**	**diff E**	**diff H**
1	6580428,484	156165,549	11,389	6580428,485	156165,548	11,403	0,001	-0,001	0,014
1	6580426,916	156170,249	11,309	6580426,916	156170,240	11,322	0,000	-0,009	0,013
1	6580427,442	156165,648	11,380	6580427,439	156165,646	11,383	-0,003	-0,002	0,003
1	6580427,926	156170,819	11,279	6580427,924	156170,812	11,295	-0,002	-0,007	0,016
1	6580427,583	156165,670	11,369	6580427,580	156165,669	11,385	-0,003	-0,001	0,016
1	6580427,959	156170,378	11,289	6580427,959	156170,371	11,305	0,000	-0,007	0,016
2	6580400,210	156236,983	10,133	6580400,211	156236,982	10,141	0,001	-0,001	0,008
2	6580400,769	156241,261	10,027	6580400,769	156241,259	10,034	0,000	-0,002	0,007
2	6580401,104	156237,161	10,151	6580401,103	156237,160	10,164	-0,001	-0,001	0,013
2	6580401,047	156241,897	10,011	6580401,049	156241,892	10,017	0,002	-0,005	0,006
2	6580400,748	156237,152	10,136	6580400,747	156237,150	10,152	-0,001	-0,002	0,016
2	6580400,707	156241,987	9,995	6580400,707	156241,980	10,014	0,000	-0,007	0,019
3	6580367,689	156325,831	8,116	6580367,684	156325,836	8,120	-0,005	0,005	0,004
3	6580366,805	156331,011	8,048	6580366,804	156331,016	8,058	-0,001	0,005	0,010
3	6580367,504	156325,836	8,102	6580367,503	156325,840	8,117	-0,001	0,004	0,015
3	6580366,944	156331,123	8,037	6580366,944	156331,123	8,053	0,000	0,000	0,016
3	6580367,248	156326,475	8,100	6580367,241	156326,480	8,106	-0,007	0,005	0,006
3	6580366,807	156330,786	8,048	6580366,800	156330,785	8,059	-0,007	-0,001	0,011
4	6580336,758	156405,737	8,180	6580336,759	156405,743	8,185	0,001	0,006	0,005
4	6580336,110	156410,736	8,383	6580336,117	156410,734	8,393	0,007	-0,002	0,010
4	6580336,591	156405,879	8,186	6580336,594	156405,881	8,190	0,003	0,002	0,004
4	6580336,481	156410,339	8,352	6580336,479	156410,342	8,362	-0,002	0,003	0,010
4	6580335,328	156405,569	8,179	6580335,325	156405,575	8,179	-0,003	0,006	0,000
4	6580336,578	156410,856	8,374	6580336,577	156410,854	8,382	-0,001	-0,002	0,008
5	6580304,454	156494,554	13,298	6580304,455	156494,564	13,308	0,001	0,010	0,010
5	6580303,586	156497,813	13,545	6580303,590	156497,815	13,554	0,004	0,002	0,009
5	6580304,326	156493,380	13,203	6580304,337	156493,392	13,217	0,011	0,012	0,014
5	6580303,631	156498,458	13,576	6580303,636	156498,463	13,588	0,005	0,005	0,012
5	6580303,867	156494,096	13,284	6580303,868	156494,109	13,286	0,001	0,013	0,002
5	6580303,708	156497,950	13,540	6580303,724	156497,954	13,553	0,016	0,004	0,013
						Average	0,001	0,001	0,010
						u(diff)	0,005	0,006	0,005
						u(average)	0,001	0,001	0,001

Appendix 4

Coordinates for the laser targets (MT1-8) estimated from the laser cloud (MMS)

	N	E	Höjd	mean-N_i	mean-E_i	mean-H_i
MT1	6580410,287	156194,041	9,703	-0,015	0,027	-0,011
MT1	6580410,270	156194,084	9,682	0,002	-0,016	0,010
MT1	6580410,273	156194,064	9,700	-0,001	0,004	-0,007
MT1	6580410,275	156194,048	9,688	-0,003	0,021	0,004
MT1	6580410,259	156194,095	9,691	0,013	-0,027	0,002
MT1	6580410,267	156194,078	9,691	0,005	-0,010	0,002
average:	**6580410,272**	**156194,068**	**9,693**			
u(sample):	0,009	0,021	0,008	0,009	0,021	0,008
u(average):	0,004	0,009	0,003			
MT2	6580423,201	156198,974	9,623	-0,005	0,004	-0,007
MT2	6580423,191	156198,994	9,619	0,004	-0,016	-0,003
MT2	6580423,203	156198,957	9,617	-0,007	0,021	-0,001
MT2	6580423,199	156198,961	9,630	-0,003	0,017	-0,014
MT2	6580423,190	156198,986	9,603	0,005	-0,008	0,012
MT2	6580423,190	156198,995	9,602	0,005	-0,018	0,014
average:	**6580423,196**	**156198,978**	**9,615**			
u(sample):	0,006	0,016	0,011	0,006	0,016	0,011
u(average):	0,002	0,007	0,005			
MT3	6580377,364	156281,141	7,588	-0,059	-0,005	-0,003
MT3	6580377,289	156281,150	7,597	0,016	-0,014	-0,011
MT3	6580377,298	156281,107	7,578	0,008	0,028	0,008
MT3	6580377,298	156281,119	7,585	0,008	0,016	0,000
MT3	6580377,286	156281,155	7,588	0,019	-0,020	-0,003
MT3	6580377,298	156281,141	7,577	0,008	-0,005	0,009
average:	**6580377,305**	**156281,136**	**7,585**			
u(sample):	0,029	0,019	0,007	0,029	0,019	0,007
u(average):	0,012	0,008	0,003			
MT4	6580390,515	156286,640	7,678	-0,009	0,002	-0,006
MT4	6580390,510	156286,622	7,660	-0,004	0,020	0,013
MT4	6580390,512	156286,618	7,678	-0,006	0,025	-0,005
MT4	6580390,502	156286,657	7,667	0,005	-0,014	0,006
MT4	6580390,499	156286,658	7,668	0,007	-0,015	0,005
MT4	6580390,500	156286,659	7,684	0,006	-0,017	-0,011
average:	**6580390,506**	**156286,642**	**7,672**			
u(sample):	0,007	0,019	0,009	0,007	0,019	0,009
u(average):	0,003	0,008	0,004			

MT5	6580345,913	156365,046	6,377	-0,003	0,005	-0,019
MT5	6580345,911	156365,053	6,352	-0,001	-0,002	0,006
MT5	6580345,911	156365,043	6,343	-0,001	0,008	0,015
MT5	6580345,921	156365,023	6,358	-0,011	0,028	0,000
MT5	6580345,906	156365,061	6,361	0,004	-0,010	-0,003
MT5	6580345,899	156365,080	6,358	0,011	-0,029	0,001
average:	**6580345,910**	**156365,051**	**6,358**			
u(sample):	0,007	0,019	0,011	0,007	0,019	0,011
u(average):	0,003	0,008	0,005			
MT6	6580360,019	156369,707	6,459	-0,012	0,029	-0,011
MT6	6580359,998	156369,761	6,446	0,009	-0,025	0,003
MT6	6580360,010	156369,718	6,460	-0,003	0,018	-0,012
MT6	6580360,011	156369,723	6,433	-0,004	0,012	0,015
MT6	6580360,000	156369,758	6,444	0,007	-0,022	0,004
MT6	6580360,004	156369,746	6,448	0,003	-0,011	0,000
average:	**6580360,007**	**156369,735**	**6,448**			
u(sample):	0,008	0,023	0,010	0,008	0,023	0,010
u(average):	0,003	0,009	0,004			
MT7	6580313,418	156451,833	8,813	-0,002	0,009	0,004
MT7	6580313,412	156451,861	8,810	0,004	-0,019	0,006
MT7	6580313,427	156451,814	8,828	-0,011	0,028	-0,011
MT7	6580313,411	156451,863	8,819	0,005	-0,021	-0,003
MT7	6580313,414	156451,859	8,819	0,002	-0,017	-0,003
MT7	6580313,414	156451,823	8,810	0,002	0,019	0,007
average:	**6580313,416**	**156451,842**	**8,817**			
u(sample):	0,006	0,021	0,007	0,006	0,021	0,007
u(average):	0,002	0,009	0,003			
MT8	6580324,596	156455,475	9,203	-0,008	0,027	-0,003
MT8	6580324,589	156455,509	9,199	-0,001	-0,008	0,001
MT8	6580324,584	156455,485	9,197	0,004	0,016	0,003
MT8	6580324,586	156455,507	9,203	0,002	-0,005	-0,003
MT8	6580324,581	156455,524	9,201	0,007	-0,022	0,000
MT8	6580324,591	156455,510	9,198	-0,003	-0,008	0,002
average:	**6580324,588**	**156455,502**	**9,200**			
u(sample):	0,006	0,018	0,002	0,006	0,018	0,002
u(average):	0,002	0,007	0,001			

where:

average	- the average of the sample
u(sample)	- standard uncertainty of unit weight of the sample
u(average)	- standard uncertainty of the average

Appendix 5

Comparison of coordinates for laser targets from positioning module and from total stations.

	diff N	diff E	fi_d	diff	diffT	diffL	diffH
MT1	-0,015	0,014	2,381	0,020	-0,009	0,018	-0,006
MT1	0,002	-0,029	-1,507	0,029	-0,008	-0,028	0,015
MT1	-0,001	-0,009	-1,647	0,009	-0,004	-0,008	-0,003
MT1	-0,003	0,007	1,978	0,008	0,000	0,008	0,009
MT1	0,013	-0,040	-1,266	0,042	-0,002	-0,042	0,006
MT1	0,005	-0,023	-1,374	0,024	-0,004	-0,024	0,006
MT2	-0,008	0,014	2,067	0,016	-0,002	0,016	-0,008
MT2	0,002	-0,006	-1,248	0,006	0,000	-0,006	-0,004
MT2	-0,010	0,031	1,872	0,032	0,002	0,032	-0,002
MT2	-0,006	0,027	1,776	0,027	0,004	0,027	-0,015
MT2	0,003	0,002	0,626	0,003	0,003	0,001	0,012
MT2	0,003	-0,007	-1,222	0,008	0,000	-0,008	0,013
MT3	-0,058	-0,022	-2,779	0,062			
MT3	0,017	-0,031	-1,075	0,035	0,005	-0,034	-0,012
MT3	0,008	0,012	0,959	0,014	0,012	0,008	0,007
MT3	0,008	0,000	-0,048	0,008	0,008	-0,003	0,000
MT3	0,020	-0,036	-1,068	0,042	0,006	-0,041	-0,003
MT3	0,008	-0,022	-1,201	0,023	0,000	-0,023	0,008
MT4	-0,009	0,003	2,829	0,010	-0,008	0,006	-0,006
MT4	-0,004	0,021	1,749	0,021	0,004	0,021	0,012
MT4	-0,006	0,025	1,793	0,026	0,003	0,026	-0,006
MT4	0,004	-0,014	-1,254	0,014	0,000	-0,014	0,005
MT4	0,007	-0,015	-1,110	0,016	0,002	-0,016	0,004
MT4	0,006	-0,016	-1,212	0,017	0,000	-0,017	-0,012
MT5	0,002	-0,004	-1,081	0,005	0,001	-0,005	-0,019
MT5	0,004	-0,011	-1,207	0,012	0,000	-0,012	0,006
MT5	0,004	-0,001	-0,165	0,004	0,004	-0,002	0,015
MT5	-0,006	0,019	1,869	0,020	0,001	0,020	0,000
MT5	0,009	-0,019	-1,117	0,021	0,002	-0,021	-0,003
MT5	0,016	-0,038	-1,172	0,041	0,002	-0,041	0,000
MT6	-0,013	0,042	1,871	0,044	0,002	0,044	-0,011
MT6	0,008	-0,012	-0,974	0,014	0,003	-0,014	0,002
MT6	-0,004	0,031	1,703	0,032	0,007	0,031	-0,012
MT6	-0,005	0,026	1,744	0,026	0,005	0,026	0,015
MT6	0,006	-0,009	-0,929	0,011	0,003	-0,010	0,004
MT6	0,002	0,003	0,949	0,003	0,003	0,002	0,000
MT7	0,002	-0,001	-0,683	0,002	0,001	-0,002	0,004
MT7	0,008	-0,029	-1,313	0,030	-0,003	-0,030	0,007
MT7	-0,007	0,018	1,971	0,019	-0,001	0,019	-0,011
MT7	0,009	-0,031	-1,290	0,033	-0,002	-0,032	-0,002

MT7	0,006	-0,027	-1,348	0,028	-0,004	-0,028	-0,002
MT7	0,006	0,009	0,954	0,011	0,009	0,006	0,007
MT8	-0,008	0,041	1,769	0,042	0,006	0,042	-0,003
MT8	-0,001	0,007	1,754	0,007	0,001	0,007	0,001
MT8	0,004	0,031	1,449	0,031	0,014	0,027	0,003
MT8	0,002	0,009	1,345	0,009	0,005	0,008	-0,003
MT8	0,007	-0,008	-0,830	0,011	0,004	-0,010	-0,001
MT8	-0,003	0,006	1,978	0,007	0,000	0,007	0,002
				Average	0,000	-0,001	0,000
				u(diff)	0,005	0,023	0,008

Appendix 6

Coordinates of the mobile platform and orientation angles

Run 1

N	E	H	DOP	NoSatellites	Roll	Pitch	Heading	u(N)	u(E)	u(H)	u(roll)	u(pitch)	u(heading)
6580428,484	156165,549	11,389	0,6	22	-0,4802	-1,8268	108,9422	0,002	0,002	0,005	0,0120	0,0120	0,1360
6580400,210	156236,983	10,133	0,6	22	0,8736	-2,7020	109,7050	0,002	0,002	0,005	0,0120	0,0130	0,1690
6580367,689	156325,831	8,116	0,6	22	-0,3544	-1,1770	110,2724	0,002	0,002	0,005	0,0130	0,0130	0,1460
6580336,758	156405,737	8,180	0,6	22	-0,3724	1,5956	110,1972	0,002	0,002	0,005	0,0130	0,0130	0,1330
6580304,454	156494,554	13,298	0,6	22	-0,9614	3,8946	109,9580	0,002	0,002	0,005	0,0120	0,0130	0,1500

Run 2

N	E	H	DOP	NoSatellites	Roll	Pitch	Heading	u(N)	u(E)	u(H)	u(roll)	u(pitch)	u(heading)
6580303,586	156497,813	13,545	0,6	22	1,0137	-4,8949	289,7097	0,002	0,002	0,005	0,0130	0,0130	0,1520
6580336,110	156410,736	8,383	0,6	22	0,1435	-3,3865	290,1930	0,002	0,003	0,005	0,0130	0,0130	0,1320
6580366,805	156331,011	8,048	0,6	22	0,5448	0,1066	290,0851	0,002	0,003	0,005	0,0130	0,0130	0,1360
6580400,769	156241,261	10,027	0,6	22	-0,3663	1,3788	290,7528	0,002	0,003	0,005	0,0130	0,0130	0,1380
6580426,916	156170,249	11,309	0,6	22	0,1561	0,1349	290,6397	0,002	0,002	0,005	0,0120	0,0130	0,1050

Run 3

N	E	H	DOP	NoSatellites	Roll	Pitch	Heading	u(N)	u(E)	u(H)	u(roll)	u(pitch)	u(heading)
6580427,442	156165,648	11,380	0,6	22	0,8534	-1,5968	109,1820	0,002	0,002	0,005	0,0120	0,0130	0,0960
6580401,104	156237,161	10,151	0,6	22	0,6766	-2,7300	110,5956	0,002	0,002	0,005	0,0120	0,0130	0,1080
6580367,504	156325,836	8,102	0,6	22	-0,0980	-1,2000	110,9740	0,002	0,003	0,005	0,0120	0,0130	0,1000
6580336,591	156405,879	8,186	0,6	22	-0,0990	1,6375	110,7290	0,002	0,003	0,005	0,0120	0,0130	0,1180
6580304,326	156493,380	13,203	0,6	22	-0,4218	4,1719	109,0290	0,002	0,003	0,005	0,0120	0,0130	0,1480

Run 4

N	E	H	DOP	NoSatellites	Roll	Pitch	Heading	u(N)	u(E)	u(H)	u(roll)	u(pitch)	u(heading)
6580303,631	156498,458	13,576	0,6	22	1,7511	-4,9851	289,4639	0,002	0,003	0,005	0,0120	0,0120	0,1200
6580336,481	156410,339	8,352	0,6	22	0,4760	-3,5410	290,8970	0,002	0,003	0,005	0,0120	0,0130	0,1090
6580366,944	156331,123	8,037	0,6	22	0,8320	-0,0660	290,5910	0,002	0,003	0,005	0,0120	0,0130	0,1130
6580401,047	156241,897	10,011	0,6	22	0,3736	1,1556	290,5730	0,002	0,003	0,005	0,0120	0,0130	0,1140
6580427,926	156170,819	11,279	0,6	22	1,5520	0,0610	290,1260	0,002	0,003	0,005	0,0120	0,0120	0,1040

Run 5

N	E	H	DOP	NoSatellites	Roll	Pitch	Heading	u(N)	u(E)	u(H)	u(roll)	u(pitch)	u(heading)
6580427,583	156165,670	11,369	0,6	22	0,8679	-1,7590	109,4034	0,002	0,003	0,005	0,0120	0,0120	0,1110
6580400,748	156237,152	10,136	0,6	22	0,9320	-2,8540	110,0380	0,002	0,003	0,005	0,0120	0,0130	0,0960
6580367,248	156326,475	8,100	0,6	22	0,0433	-1,3706	110,2997	0,002	0,003	0,005	0,0120	0,0130	0,1020
6580335,328	156405,569	8,179	0,6	22	1,2048	1,5702	109,7606	0,002	0,003	0,005	0,0120	0,0130	0,1190
6580303,867	156494,096	13,284	0,6	22	0,5590	3,8002	110,0832	0,002	0,003	0,005	0,0120	0,0130	0,1300

Run 6

N	E	H	DOP	NoSatellites	Roll	Pitch	Heading	u(N)	u(E)	u(H)	u(roll)	u(pitch)	u(heading)
6580303,708	156497,950	13,540	0,6	22	1,4525	-5,0095	288,5340	0,002	0,003	0,005	0,0120	0,0120	0,1260
6580336,578	156410,856	8,374	0,6	22	0,6632	-3,6242	290,3364	0,002	0,003	0,005	0,0120	0,0120	0,1150
6580366,807	156330,786	8,048	0,6	22	0,7070	0,0256	289,7796	0,002	0,003	0,005	0,0120	0,0120	0,1160
6580400,707	156241,987	9,995	0,6	22	0,0713	1,1980	290,0450	0,002	0,003	0,005	0,0120	0,0120	0,1070
6580427,959	156170,378	11,289	0,6	22	1,4919	0,1480	290,4898	0,002	0,003	0,005	0,0120	0,0120	0,0960

where:

DOP	Dilution Of Precision,
NoSatellites	Number of Satellites,
u(*)	standard uncertainty of the given parameter

7. Abbreviations

GNSS	Global Navigation Satellite System
IMU	Inertial Measuring Unit
INS	Inertial Navigation System
MMS	Mobile Mapping System
RTK	Real Time Kinematics
SWEPOS	Swedish continuously operated reference GNSS stations
TS	Total Station